A Particle Tracking Velocimetric Study of Stress Relaxation Behavior of Entangled Polystyrene Solutions after Stepwise Shear

ARTICLE *in* MACROMOLECULES · AUGUST 2012

Impact Factor: 5.8 · DOI: 10.1021/ma3010026

2 AUTHORS:

Gengxin Liu
University of Akron
8 PUBLICATIONS **33** CITATIONS
SEE PROFILE

Shi-Qing Wang
University of Akron
257 PUBLICATIONS **5,011** CITATIONS
SEE PROFILE

Macromolecules

Note

pubs.acs.org/Macromolecules

A Particle Tracking Velocimetric Study of Stress Relaxation Behavior of Entangled Polystyrene Solutions after Stepwise Shear

Gengxin Liu and Shi-Qing Wang*

Department of Polymer Science, University of Akron, Akron, Ohio 44325

Supporting Information

I. INTRODUCTION

Since the arrival of the Doi−Edwards tube model for polymer rheology[1−4] there have been numerous experimental studies performed to validate the model. The most well-known agreement between the theory and experiment in the nonlinear regime involves the stress relaxation behavior after stepwise shear. The tube model anticipates two-step relaxation dynamics for well-entangled polymers after a large step strain. Specifically, there would be a kink in the time dependence of the relaxing stress.[5] The sharp stress drop would occur quiescently around the Rouse relaxation time τ_R due to the chain retraction, which is assumed in the tube model to take place in a barrier-free manner. This ansatz of the tube model has the consequence that the chain orientation would relax on the time scale of reptation, decoupled from the fast dynamics associated with chain stretching. Thus, the structure of the tube model automatically insures that there would be time-strain separability, i.e., the relaxing stress would have the same time dependence beyond the Rouse time τ_R, independent of the magnitude of the applied step strain. In particular, the strain softening would take place, due to the assumed barrier-free chain retraction. In other words, the residual shear stress arises entirely from the surviving chain orientation

$$\sigma(\gamma, t) = G_{eq}(t)\gamma h(\gamma), \quad \text{for } t > \tau_R \tag{1}$$

so that the relaxation modulus $G(\gamma,t) = G_{eq}(t)h(\gamma)$ actually decreases with the magnitude of γ beyond a certain value of γ. Here the damping function $h(\gamma)$ depicts the strain softening as[2]

$$h(\gamma) = G(\gamma, t)/G_{eq}(t) \cong 1/(1 + \gamma^2/5), \quad \text{for } t > \tau_R \tag{2}$$

where $G_{eq}(t)$ is the equilibrium relaxation modulus that describes the stress relaxation $\sigma(t)$ in the regime of linear response, i.e., $\sigma(t) = G_{eq}(t)\gamma$, for $\gamma \ll 1$.

Experimental reports of stress relaxation behavior first appeared in the 1970s.[6−8] The systems under study were typically polystyrene solutions capable of undergoing wall slip.[9−12] Such solutions indeed show two-step relaxation upon large stepwise strain in misleading agreement with the theoretical depiction based on the Doi−Edwards tube model.[5] Some of the sharp stress decline was actually so severe that the data showed ultra strain softening, deviating downward from eqs 1 and 2, such as those of Osaki and co-workers[13] in 1980 and of Vrentas and Graessley[14] in 1982. But a subsequent 1982 paper from Osaki's lab[15] produced stress relaxation behavior in quantitative agreement with the tube model prediction. It is this match between the experiment and theory that is well-known in the community[5] and hailed as the great triumph of the tube model.

In the past 40 years, there have been two dozens publications on step strain of entangled polystyrene (PS) solutions,[6−11,13,15−31] making the PS solutions a classical system to study nonlinear rheology of entangled polymers. Whenever the data were in disagreement with the tube model, it was suggested[10,11] that wall slip or other material instabilities or even instrument limitations were the causes. Indeed, in the case of ultra strain softening,[14] wall slip could be the origin of the steep stress decline at short times, leading to the two-step characteristic. But we were still left with the question of whether we fully understand the nature of the nonlinear responses when there is agreement between experiment and theory given by the damping function of eq 2.

Nearly all of the two dozen papers[6−11,13,15−31] and other studies on other polymer solutions measured the damping function to compare with eq 2 instead of presenting the raw data of the actual relaxing stress as a function of time. We were never warned that even the normal strain softening, as defined by eqs 1 and 2 and known as type B behavior,[10] already involves too much softening. In other words, any data in agreement with the damping function of eq 2 would suggest that at long times ($t > t_k$) the residual shear stress actually shows a maximum at $\gamma > \sqrt{5}$ and eventually declines as $1/\gamma$, as described by eq 1 along with eq 2. When the experimental data of $\sigma(\gamma, t > t_k)$ actually obeys eq 1, showing a decrease with γ, we were alarmed and prompted to apply a particle-tracking velocimetric technique (PTV) in conjunction with the simultaneous rheometric measurements to answer the following questions. Did the reduced shear stress reflect a breakdown of the strained entanglement network? For well-entangled polymer solutions, could such a structural breakdown take place homogeneously?

On the basis of several entangled polybutadiene solutions, the recent PTV observations revealed[32] that the stress relaxation after a sizable stepwise shear was nonquiescent, contradicting the wide-held perception that a shear-strained polymeric liquid should always relax quiescently upon shear cessation. A subsequent PTV study confirmed that macroscopic motions were still present during stress relaxation even when the imposed stepwise shear occurred at a rate too low according to the tube model to produce chain stretching.[33]

Received: May 17, 2012
Revised: June 28, 2012
Published: August 7, 2012

dx.doi.org/10.1021/ma3010026 | Macromolecules 2012, 45, 6741−6747

The objective of the present study is to determine whether the previously observed nonquiescent relaxation is universal, in particular, whether the classical system of entangled polystyrene solutions[6−11,13,15−31] would also show macroscopic motions during stress relaxation if they are sufficiently entangled and possessive of a sizable slip length b.[34]

II. EXPERIMENTAL SECTION

A. Materials. Entangled polystyrene (PS) solutions were prepared by first dissolving a desired wt % of high molecular weight polystyrene in carbon disulfide. To this solution either tricresyl phosphate (TCP) or diethyl phthalate (DEP) was added to form a uniform solution. All previous PS solutions solutions[6−11,13,15−31] used to study stress relaxation behavior were based on either TCP or DEP. For the present study, we prepared three solutions: two made of 7 volume % of PS-20 M in TCP and DEP respectively, and the other of 20 volume % PS-2 M in TCP. They are labeled as PS20M(7%-TCP), PS20M(7%-DEP) and PS2M(20%-TCP) respectively. Table 1 lists the basic information about the materials used in the present study.

Table 1. Molecular Characteristics of PS and Solvents

sample	M_n	source	M_w/M_n	η (Pa·s)
PS-20M	20 000 000	Polymer Standard	1.20	
PS-2M	2 000 000	Pressure Chemical	1.30	
polystyrene-20K	19 600	Polysciences	1.05	
TCP (tricresyl phosphate)	368.37	Aldrich 1330−78−5		0.1
DEP (diethyl phthalate)	222.24	Aldrich 84−66−2		0.012

The silver-coated particles (HGS-10) from Dantec Dynamics are polydisperse with the diameter ranging from 5 to 30 μm. They were first ultrasonicated in CS_2 and then added to the PS solutions. The final loading of the particles was at a level of 200−500 ppm. Since the vapor pressure of TCP and DEP are rather high, carbon disulfide can readily evaporate under ambient conditions for nearly a week under a hood. The remaining carbon disulfide was removed in vacuum oven over several days.

B. Apparatuses. Step shear experiments of PS-20M solutions were carried out on an Advanced Rheometric Expansion System (ARES) using a cone-plate geometry with diameter of 25 mm and cone angle of 4 deg. The particle-tracking velocimetric (PTV) setup on ARES as depicted in Figure 1 allows simultaneous determination of the rheometric information and corresponding deformation field and is a key apparatus in the present study. The surfaces of the cone and plate were covered with black sand papers to suppress wall slip and to minimize light reflection during the PTV observation, except for the PTV glass window. The sand paper was Waterproof silicon carbide

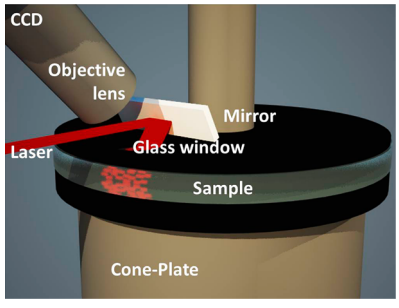

Figure 1. Schematic configuration of the PTV setup. Black plate on the bottom side is the rotating plate while the black top is stationary, connected to the torque transducer.

P1000 Grid. Past studies have shown[17,34,35] that topographically rough surface improves the mechanical coupling between the sample and shearing surfaces. The present study also revealed the effect of surface condition.

The PTV experiments on the PS2M(20%-TCP) solution were carried out on an Anton Paar MCR301 rotational rheometer based on parallel-plate geometry with diameter of 25 mm and a gap of 1 mm. The PTV setup on MCR301 involves wrapping a transparent PET film around the meniscus with the CCD camera peeking horizontally through the film, as depicted previously.[32] No sand papers were used in the parallel-plate setup.

In the PTV setup, the silver-coated particles embedded in the sample are illuminated by a sheet of laser light(cross-section 2 mm by 0.15 mm). The laser beam was incident into the sample at an appropriate angle as shown in Figure 1 so that a CCD camera (30 frames per second) can record through the same optical window. Movements of the particle were recorded by a Toshiba DR 430 recorder onto a DVD disk. To have a field of view around 1.5 mm by 1 mm, a DIN objective lens (3.2×) was mounted on the CCR camera through an adaptive tube (Edmund Optics: U54−868). The distance traveled by a particle can be determined frame by frame using Ulead VideoStudio SE DVD software. These PTV observations were made at a radial distance of 4 mm from the edge. The spatial resolution of our PTV is around 30 μm.

To make stepwise shear, we employ different protocols, including the stress relaxation mode where the prescribed strain of various magnitudes is applied within the same amount of time ca. 0.04 s, and a truncated startup shear that produces the various strains at the same shear rate.

C. Characterization of Linear Viscoelastic Properties. Small-amplitude oscillatory shear (SAOS, strain amplitude γ = 4%) measurements were carried out to determine linear viscoelastic properties of these PS solutions based on an Anton Paar MCR301 rotational rheometer coupled to a cone-plate assembly with 25 mm diameter and 2 ° cone angle. Parts a and b of Figure 2, respectively, show the storage and loss moduli as a function of the oscillation frequency ω for the two solutions of PS20M(7%-TCP) and PS2M(20%-TCP). From such SAOS measurements the basic linear viscoelastic properties such as the elastic plateau modulus G_{pl}, the reptation time τ_d, and zero-frequency viscosity η_0, can be obtained as listed in Table 2 including the reptation time or terminal relaxation time τ and the Rouse relaxation time τ_R.

In particular, the Rouse relaxation time τ_R can be estimated in two ways, related either to the zero-shear viscosity η or to the frequency dependence of storage modulus G' in the Rouse regime.[36,37] Specifically, we employ the following two formulas[20] in our evaluation of τ_R:

$$\tau_R = \frac{6M\eta}{\pi^2 cRT}\left(\frac{M_c}{M}\right)^{2.4} \tag{4}$$

and

$$\tau_R = \left(\frac{aM}{1.111cRT}\right)^2 \tag{5}$$

We also need to estimate the sample's ability to undergo wall slip by evaluating the slip length b according to

$$b = (\eta/\eta_i)a \tag{6}$$

where η is the zero-shear solution viscosity, η_i is the viscosity at the polymer/wall interface in absence of chain entanglement between adsorbed and unbound bulk chains, and the thickness of the entanglement-free interfacial layer a is the entanglement spacing of the PS solution, which can be related[38] to the entanglement spacing l_{ent} of the pure PS melt and the polymer volume ϕ fraction in the solution as $a = l_{ent}\phi^{-2/3}$. Here the entanglement spacing l_{ent} is 7.2 nm for the PS melt.[38−40] Since PS slows down the solvent dynamics, we cannot use the solvent viscosity as the interfacial viscosity η_i. We prepared two solutions based on a lower molecular weight PS as listed

dx.doi.org/10.1021/ma3010026 | Macromolecules 2012, 45, 6741−6747

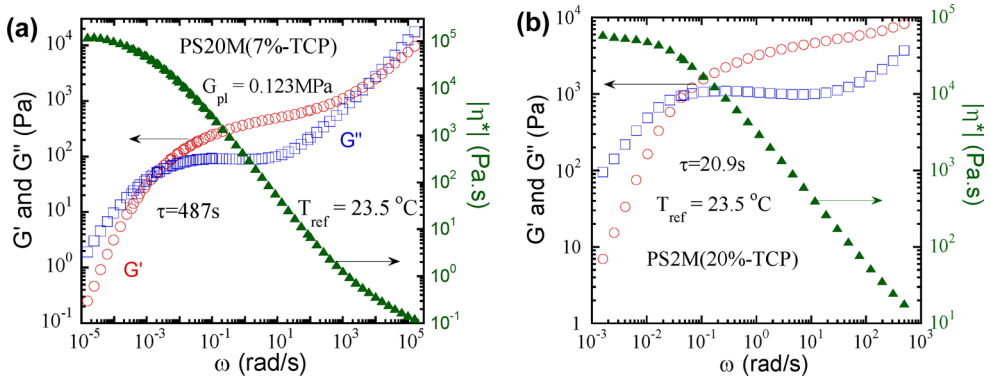

Figure 2. (a) Small amplitude oscillatory shear measurements of storage (red circles, G'), loss moduli (blue squares, G''), and the complex viscosity, green solid triangles, $|\eta^*|$, as a function of frequency ω, for (a) PS20M(7%-TCP) and (b) PS2M(20%-TCP).

Table 2. Linear Viscoelastic Characteristics of the PS Solutions

solution samples	φ, Z	τ_d (s), τ_R (s)	G_{pl} (Pa)	η_0 (Pa·s)	b (mm)
PS20M(7%-TCP)	0.07, 50	487, 3.68,[a] 4.88[b]	447	122 940	3.8
PS2M(20%-TCP)	0.20, 19	17.50, 0.278[a]	4700	40 000	0.11
PS20M(7%-DEP)	0.065, 42	15.0	353		
PS19.6K(20%-TCP)				2.58	
PS19.6K(7%-TCP)				0.23	

[a]Calculated based on eq 4. [b]Calculated based on eq 5.

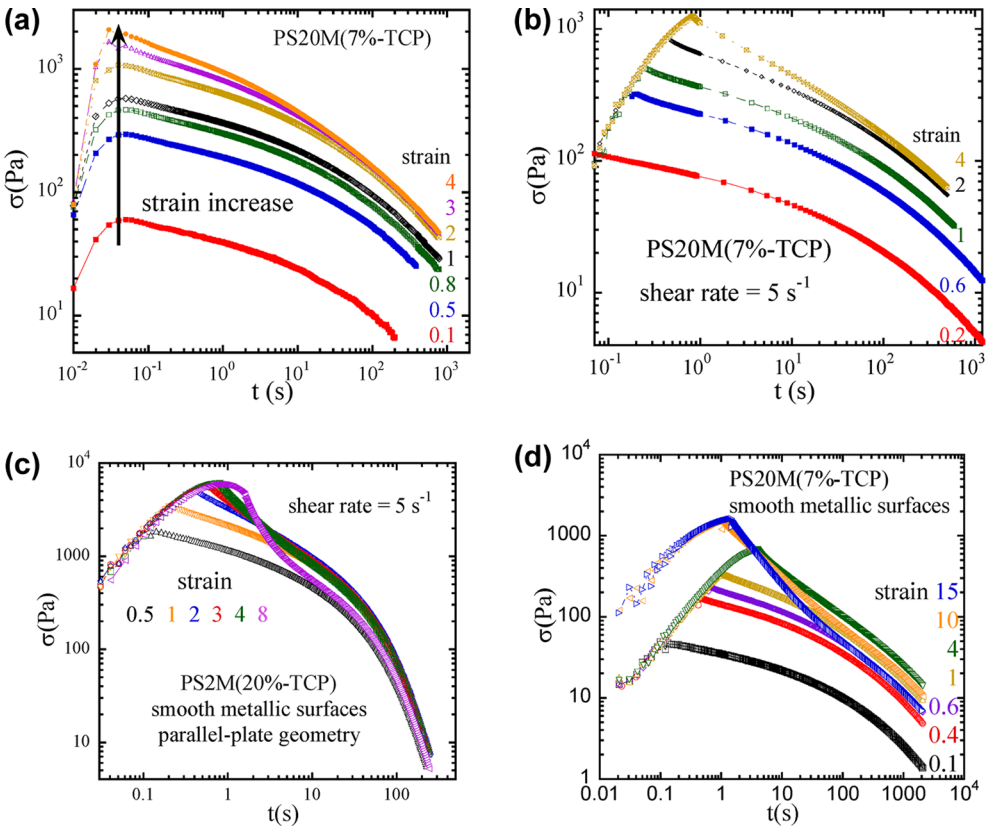

Figure 3. (a) Shear stress growth and relaxation of PS20M(7%-TCP) during and after discrete step shearing of different magnitudes by a similar time of 0.04 s, where the effective shear rate ranges from 2 to 100 s^{-1}. (b) Shear stress growth and relaxation PS20M(7%-TCP) during and after discrete step shearing of different magnitudes with same shear rate of 5 s^{-1}, corresponding to a Weissenberg number Wi = 2435. In parts a and b, the shearing surfaces are sand papers. (c) Shear stress growth and relaxation of PS2M(20%-TCP) during and after discrete step shearing of different magnitudes with the same shear rate of 5 s^{-1}, corresponding to Wi = 88. (d) Shear stress growth and relaxation of PS2M(20%-TCP) during and after discrete step shearing of different magnitudes at two different shear rates of 1 and 10 s^{-1} respectively. In parts c and d, the shearing surfaces are smooth and metallic.

dx.doi.org/10.1021/ma3010026 | Macromolecules 2012, 45, 6741−6747

in Table 2 and measured their viscosity as listed in Table 1 to be used as η_i in eq 6. The estimated values of b are the upper bounds.

III. RESULTS AND DISCUSSION

A. Stress Relaxation from Conventional Rheometry. The aim of this study to characterize the nature of the stress relaxation behavior of entangled polystyrene solutions that are very similar to those studied in the past by rheometric measurements. However, the present study differs from those of the past[6−11,13,15−31] in that the rheometric measurements are coupled with *in situ* PTV observations of the deformation field. Moreover, most of our measurements involved cone-plate and sand papers as the shearing surfaces. When either smooth steel surfaces are used or parallel-plate geometry is involved, we explicitly indicate such conditions within the figures.

Our first experiment adopts the standard protocol used to study stress relaxation. In this stress relaxation mode, the prescribed strain is produced within a very short period around 0.04 s on the ARES rheometer. In a second experiment, we use a fixed shear rate to produce the prescribed strains. This amounts to terminating a startup shear test and conducting stress relaxation upon the shear cessation. For the PS20M(7%-TCP) solution that has a reptation time τ = 487 s, a shear rate of 5 s^{-1} is exceedingly fast, corresponding to a Weissenberg number of 2435. Parts a and b of Figure 3 respectively show the shear stress as a function of time during the stepwise shear and after shear cessation, involving the two different ways to produce the prescribed strains. A similar solution based on DEP as the solvent, i.e., PS20M(7%-DEP), shows the same trend. We omit the actual stress relaxation data to spare some space. It is clear that the relaxing stress at any given time is only higher for a higher imposed strain within the explored strain range, deviating significantly from the type B behavior depicted by eq 1. Osaki classified this as type A behavior.[10] Note that these experiments involved sand papers glued onto the shearing surface of cone-plate to minimize any possible wall slip.

In contrast, for the less entangled solution of PS2M(20%-TCP), no sand papers were used to shear the sample. Shearing to different strain amplitude at a shear rate of 5 s^{-1}, involves Wi = 88, Figure 3c shows the actual stress build-up and relaxation data as a function of time for the various strain amplitude from 0.5 to 8. Contrary to Figure 3b, the shear stress at the long times is lower for γ = 4 than for γ = 2 in Figure 3c.

Thus, it appears clear that the surface condition plays a role in these nonlinear relaxation experiments. To illustrate this effect, the same PS-20M(7%-TCP) was stepwise sheared, based on smooth metallic plates. Figure 3d presents the stress build-up and relaxation data for seven different strains, ranging from 0.1 to 15, where for the two highest strains, a shear rate of 10 s^{-1} was used to ensure that the stepwise shear was completed fast enough relative to the reptation time τ.

From plots such as Figure 3a-d we can extract the damping function according to its definition given by the first equality in eq 2. Figure 4 shows the damping function obtained from the four stepwise shear experiments. It is interesting to note that the more entangled solution of PS20M(7%-TCP) shows weaker strain softening when the sander papers were used as the shearing surfaces. In other words, for smooth steel surfaces the solution produces strain softening that falls onto the DE damping function, whereas the same solution show type A behavior[10] in presence of sand papers. For PS solutions, it was found that the product of polymer concentration c (proportional to the weight fraction ϕ) and molecular weight M

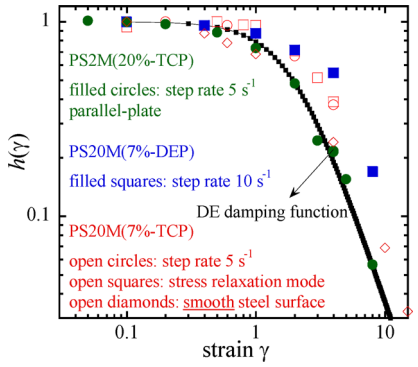

Figure 4. Damping function h that represents the normalized stress relaxation at long times from the different tests involving different methods and different solution samples, along with the Doi−Edwards damping function as the thin line with small squares.

dictates whether a sample can be described by the DE damp function of eq 2 or not. Normally, a PS solution with higher cM is more strain softening. Specifically, it was reported[8] that the experimental data were consistent with the tube model calculation of eq 2 only for $cM < 10^6$, corresponding to a relatively weak level of chain entanglement. When $cM > 10^6$, the solutions typically showed type C behavior, i.e., ultra strain softening, with their damping function deviating downward from the DE damping function of eq 2. Indeed, the PS2M(20%-TCP) satisfies $cM < 10^6$ and happens to display its damping function in agreement with eq 2 though we caution that this set of data was collected with parallel-plate and therefore cannot be quantitatively compared with the tube model. On the other hand, PS20M(7%-TCP) meets the condition of $cM > 10^6$. But instead of type C behavior[10] found in the literature that usually involve smooth metallic plates, we observed type A behavior, i.e., the (open and filled) squares and circles are above the DE damping function. We attribute this to the use of sand papers as the shearing surfaces.

B. *In Situ* PTV Observations Revealing Nonquiescent Relaxation. To explore the nature of the observed stress relaxation behavior, we conducted simultaneous PTV observations corresponding to the actual rheometric data presented in Figure 3a−c. We first present the PTV measurements after the various stepwise shear depicted in Figure 3c. Figure 5 shows that the stress relaxation depicted in Figure 3c did not occur quiescently. Without use of the sand papers as the shearing surfaces, the step-strained PS2M(20%-TCP) appeared to have suffered "arrested" wall slip[41] at the low strain of 2 as well as internal breakup at the high strains. In other words, the strained solution showed some failure at the sample/stationary-plate upon shear cessation for γ = 2. There were also significant motions in the bulk at γ = 3 and 4. Such breakup greatly relieved the residual shear stress and produced the strain softening shown in Figure 3c and Figure 4. Similarly, the stress relaxation of the PS20M(7%-TCP) solution also involved macroscopic motions as shown in Figure 6. Nonquiescent relaxation is obvious in the first 60 s.

C. Motions Inside and Outside. Admittedly, the experimental setup was imperfect in the sense it is a finite system, with a rim of free surface at the edge. Edge instability could complicate nonlinear rheological experiments. However, it is not an issue for the present step strain experiments because there is no edge fracture during the stepwise shear. Specifically, the PTV observations of the edge indicate a uniform

dx.doi.org/10.1021/ma3010026 | *Macromolecules* 2012, 45, 6741−6747

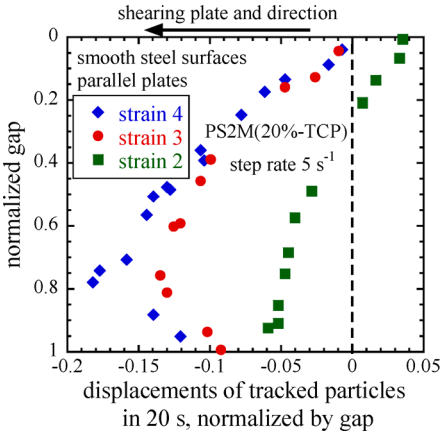

Figure 5. Particle-tracking velocimetric (PTV) detection of macroscopic motions after various discrete step strains, showing the displacements of tracked particles during a period of 20 s immediately after shear cessation. The displacements are normalized by the gap distance. Quiescent relaxation was found for strain equal to 1 and below.

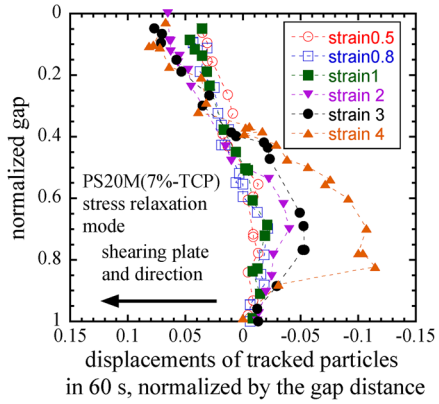

Figure 6. Particle-tracking velocimetric (PTV) detection of macroscopic motions after various discrete step strains, showing the displacements of tracked particles during a period of 60 s immediately after shear cessation. The displacements are normalized by the gap.

deformation field up to the point of shear cessation. Moreover, during the stress relaxation the PTV observations only detected weaker macroscopic motions on the rim than inside the sample.

Specifically, we set up two cameras to observe both inside the sample and at the edge during stress relaxation for two discrete stepwise shear tests of the PS20M(7%-TCP) solution. Figure 7 show that there were the greater motions inside the sample than there were at the edge. Thus, this result is consistent with a previous conclusion[42] that the nonquiescent relaxation took place without any edge instability. The previous study built and employed a special costumer-made cone-plate apparatus to ensure that during the large step strain the edge did not suffer sufficient strain and remained motionless.[42]

D. Nonquiescent Relaxation at $Wi_R < 0.1$. Conventional step strain involves the application of the stress relaxation mode, i.e., to achieve the prescribed strain amplitude within a period negligibly shorter than the reptation time τ. Thus, step strain would definitely involve chain stretching. The strain softening shown in eq 1 and eq 2 occurs because the fast barrier-free chain retraction would take place on the Rouse time scale according to the tube model. The preceding stepwise strain experiments revealed macroscopic motions upon shear

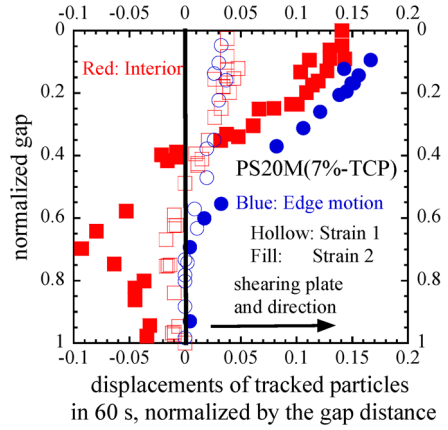

Figure 7. Particle-tracking velocimetric (PTV) detection of macroscopic motions going on both inside the cone-plate as well as on the free-surface edge.

cessation. This was not anticipated by the tube theory because the chain retraction was thought to occur uniformly while the chain entanglement is preserved to ensure quiescent relaxation.

We may note that numerical efforts (Adams PRL 2009, Wang PRL2009, Adams PRL2009, JOR 2011) have been made based on some version of the tube model. However, any discussion of their merits is beyond the scope of the present work and will be provided elsewhere. In this subsection, we consider a slowly produced stepwise shear involving a rate so low that there would be no chain stretching according to the tube model. Consequently, there should not be any chain retraction during the stress relaxation, eliminating any molecular mechanism conceivable within the tube model framework to explain nonquiescent relaxation. In other words, after cessation from a stepwise shear involving a shear rate of 0.02 s^{-1} corresponding to a Weissenberg number Wi = 9.7 and Rouse−Weissenberg number (the product of shear rate times Rouse time) Wi_R = 0.074, as shown Figure 8a, the stress relaxation should be quiescent according to the tube model. However, our *in situ* PTV observations show considerable motions after shear cessation as shown in Figure 8b.

E. Inhomogeneity in LAOS. Well-entangled polymers with appreciable slip length undergo strain localization as an effective way to respond to large deformation that causes yielding through chain disentanglement. To show that there is nothing special about the present PS solutions, we also carried out large amplitude oscillatory shear (LAOS) experiments. Figure 9a shows the steady-state Lissajous plots corresponding to strain amplitude ranging from 1 to 3. Our *in situ* PTV observations confirm that there is shear banding during the LAOS as shown in Figure 9b, similar to previous PTV observations of polybutadiene solutions.[43] Thus, homogeneous shear may not be a correct assumption for entangled polymeric systems under LAOS. When there is shear banding, theoretical analysis of LAOS[44−46] becomes invalid.

CONCLUSION

Entangled polystyrene solutions have been studied in the past four decades in terms of their stress relaxation behavior[6−11,13,15−31] and compared with the theoretical description based on the tube model.[5] In fact, these previous studies have built a consensus that the tube model is a successful molecular theory for not only linear viscoelastic properties but also nonlinear rheological behavior of entangled polymers. Specif-

dx.doi.org/10.1021/ma3010026 | Macromolecules 2012, 45, 6741−6747

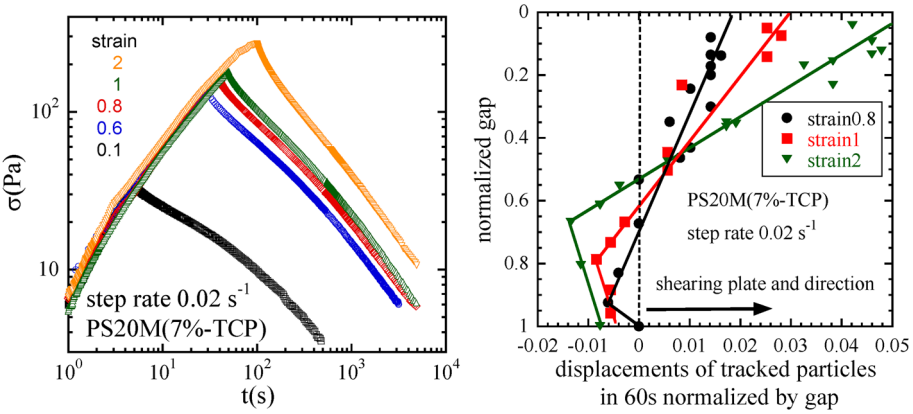

Figure 8. (a) Shear stress growth and relaxation during and after discrete step shearing of different magnitudes at a low shear rate 0.02 s^{-1}, where the Rouse Weissenberg number is less than 0.1. (b) Particle-tracking velocimetric (PTV) detection of macroscopic motions after various discrete step strains, showing the displacements of tracked particles during a period of 60 s immediately after shear cessation. The displacements are normalized by the gap distance.

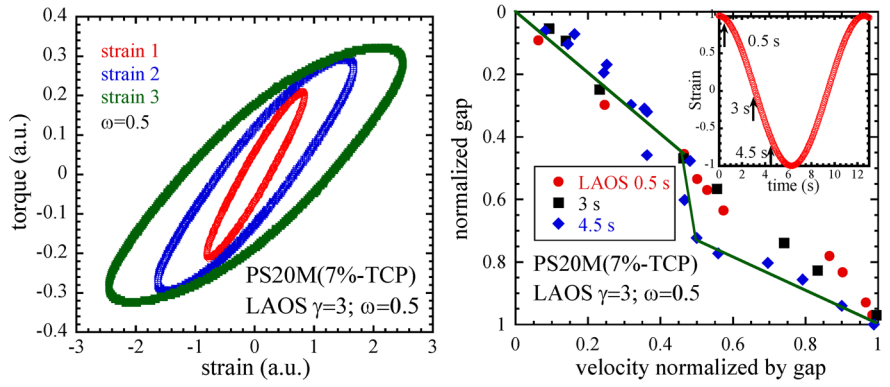

Figure 9. (a) Lissajous plots in steady state, where sand papers were used as the shearing surface. (b) Particle-tracking velocimetric (PTV) measurements of the velocity field at different moments of a cycle during LAOS in steady state. The magnitude of the velocity is normalized by the gap distance.

ically, the agreement between *some* data and the theoretical damping function[5,15] has been regarded as the validation of the tube theory despite the fact that a significant fraction of the data shows deviation from the theoretical formula of eq 1 and 2.

The present work is the first PTV study of the entangled PS solutions to show that they are not different from the other entangled polymer solutions.[32] Although the PS is not monodisperse in the molecular weight distribution (MWD), the MWD is not too broad to suppress strain localization. Consistent with the previous PTV studies of other solutions,[32] the classical PS solutions (a) also undergo nonquiescent relaxation after stepwise shear and (b) show stress relaxation behavior that deviates significantly from the tube model description. The macroscopic motions during stress relaxation affect the stress decay in a way that cannot be depicted by the tube model since the damping function is obtained under the condition of quiescent relaxation. Also consistent with a past experiment,[33] we observed nonquiescent relaxation even for a stepwise strain that was imposed so slowly that there would be no chain stretching according to the tube model. In absence of chain stretching, there would be no chain retraction after shear cessation to explain the emergence of nonquiescent relaxation within the framework of the tube model. The observed macroscopic motions seem to suggest that even this slowly imposed step shear involves significant chain stretching. It is the elastic retraction associated with the chain stretching that overcome the cohesion or entropic barrier associated with the chain entanglement.[47] The future work may need to directly probe the question of whether chain retraction could occur in a barrier-free manner on the Rouse time scale.

■ ASSOCIATED CONTENT

Ⓢ Supporting Information

A typical particle-tracking velocimetric movie of PS20M(7%-TCP) during and after a stepwise shear of amplitude strain = 4, produced in the stress relaxation mode that completed the step shear in 0.04 s. White dots are the PTV particles. The movie shows that after such a step-wise shear, the interior of the sample did not relax quiescently. The segment of the movie showing motions after shear cessation has been sped up by a factor of 100. This material is available free of charge via the Internet at http://pubs.acs.org.

■ AUTHOR INFORMATION

Corresponding Author

*E-mail: swang@uakron.edu

Notes

The authors declare no competing financial interest.

■ ACKNOWLEDGMENTS

The work is, in part, supported by the National Science Foundation (DMR-0821697).

REFERENCES

(1) Doi, M.; Edwards, S. F. *J. Chem. Soc., Faraday Trans. 2* **1978**, *74*, 1789.
(2) Doi, M.; Edwards, S. F. *J. Chem. Soc., Faraday Trans. 2* **1978**, *74*, 1818.
(3) Doi, M.; Edwards, S. F. *J. Chem. Soc., Faraday Trans. 2* **1978**, *74*, 1802.
(4) Doi, M.; Edwards, S. F. *J. Chem. Soc., Faraday Trans. 2* **1979**, *75*, 38.
(5) Doi, M.; Edwards, S. F. *The Theory of Polymer Dynamics*. Oxford University Press: Oxford, U.K., 1986.
(6) Einaga, Y.; Osaki, K.; Kurata, M.; Kimura, S.; Tamura, M. *Polym. J. (Tokyo, Jpn.)* **1971**, *2*, 550.
(7) Einaga, Y.; Osaki, K.; Kimura, S.; Yamada, N.; Tamura, M.; Kurata, M. *Polym. J. (Tokyo, Jpn.)* **1973**, *5*, 91.
(8) Fukuda, M.; Osaki, K.; Kurata, M. *J. Polym. Sci., Part B: Polym. Phys.* **1975**, *13*, 1563.
(9) Archer, L. A.; Chen, Y. L.; Larson, R. G. *J. Rheol.* **1995**, *39*, 519.
(10) Osaki, K. *Rheol. Acta* **1993**, *32*, 429.
(11) Venerus, D. C. *J. Rheol.* **2005**, *49*, 277.
(12) Archer, L. A.; Larson, R. G.; Chen, Y.-L. *J. Fluid Mech.* **1995**, *301*, 133.
(13) Osaki, K.; Kurata, M. *Macromolecules* **1980**, *13*, 671.
(14) Vrentas, C. M.; Graessley, W. W. *J. Rheol.* **1982**, *26*, 359.
(15) Osaki, K.; Nishizawa, K.; Kurata, M. *Macromolecules* **1982**, *15*, 1068.
(16) Archer, L. A. *J. Rheol.* **1999**, *43*, 1555.
(17) Archer, L. A.; Sanchez-Reyes, J.; Juliani. *Macromolecules* **2002**, *35*, 10216.
(18) Inoue, T.; Osaki, K. *J. Soc. Rheol. Jpn.* **2003**, *31*, 207.
(19) Inoue, T.; Uematsu, T.; Yamashita, Y.; Osaki, K. *Macromolecules* **2002**, *35*, 4718.
(20) Inoue, T.; Yamashita, Y.; Osaki, K. *Macromolecules* **2002**, *35*, 1770.
(21) Islam, M. T.; Archer, L. A. *J. Polym. Sci., Part B: Polym. Phys.* **2001**, *39*, 2275.
(22) Islam, M. T.; Sanchez-Reyes, J.; Archer, L. A. *J. Rheol.* **2001**, *45*, 61.
(23) Larson, R. G.; Khan, S. A.; Raju, V. R. *J. Rheol.* **1988**, *32*, 145.
(24) Morrison, F. A.; Larson, R. G. *J. Polym. Sci., Part B: Polym. Phys.* **1992**, *30*, 943.
(25) Osaki, K.; Kimura, S.; Kurata, M. *J. Polym. Sci., Part B: Polym. Phys.* **1981**, *19*, 517.
(26) Osaki, K.; Kimura, S.; Nishizawa, K.; Kurata, M. *Macromolecules* **1981**, *14*, 455.
(27) Osaki, K.; Takatori, E.; Tsunashima, Y.; Kurata, M. *Macromolecules* **1987**, *20*, 525.
(28) Osaki, K.; Watanabe, H.; Inoue, T. *Macromolecules* **1996**, *29*, 3611.
(29) Sanchez-Reyes, J.; Archer, L. A. *Macromolecules* **2002**, *35*, 5194.
(30) Venerus, D. C.; Nair, R. *J. Rheol.* **2006**, *50*, 59.
(31) Wen, Y. H.; Hua, C. C. *J. Rheol.* **2009**, *53*, 781.
(32) Ravindranath, S.; Wang, S. Q. *Macromolecules* **2007**, *40*, 8031.
(33) Boukany, P. E.; Wang, S. Q.; Wang, X. *Macromolecules* **2009**, *42*, 6261.
(34) Ravindranath, S.; Wang, S. Q.; Olechnowicz, M.; Chavan, V. S.; Quirk, R. P. *Rheol. Acta* **2011**, *50*, 97.
(35) Mhetar, V.; Archer, L. A. *Macromolecules* **1998**, *31*, 8617.
(36) Osaki, K.; Uematsu, T.; Yamashita, Y. *J. Polym. Sci., Part B: Polym. Phys.* **2001**, *39*, 1704.
(37) Osaki, K.; Inoue, T.; Isomura, T. *J. Polym. Sci., Part B: Polym. Phys.* **2000**, *38*, 1917.
(38) Colby, R. H.; Rubinstein, M. *Macromolecules* **1990**, *23*, 2753.
(39) Fetters, L. J.; Lohse, D. J.; Richter, D.; Witten, T. A.; Zirkel, A. *Macromolecules* **1994**, *27*, 4639.
(40) Fetters, L. J.; Lohse, D. J.; Colby, R. H. Chain Dimensions and Entanglement Spacings. In *Physical Properties of Polymers Handbook*, 2nd ed.; Mark, J. E., Ed.; Springer: Berlin, 2007.
(41) Boukany, P. E.; Wang, S. Q. *Macromolecules* **2009**, *42*, 2222.
(42) Li, X.; Wang, S. Q. *Rheol. Acta* **2010**, *49*, 985.
(43) Ravindranath, S.; Wang, S. Q. *J. Rheol.* **2008**, *52*, 341.
(44) Cho, K. S.; Hyun, K.; Ahn, K. H.; Lee, S. J. *J. Rheol.* **2005**, *49*, 747.
(45) Ewoldt, R. H.; Hosoi, A. E.; McKinley, G. H. *J. Rheol.* **2008**, *52*, 1427.
(46) Yu, W.; Wang, P.; Zhou, C. *J. Rheol.* **2009**, *53*, 215.
(47) Wang, S. Q.; Ravindranath, S.; Wang, Y. Y.; Boukany, P. E. *J. Chem. Phys.* **2007**, *127*, 06493.